Relative influences of multiple sources of uncertainty on cumulative and incremental tree-ring-derived aboveground biomass estimates

Postprint version

Alexander, M. R., Rollinson, C. R., Babst, F., Trouet, V., & Moore, D. J. P.

Published in: Trees

Reference: Alexander, M. R., Rollinson, C. R., Babst, F., Trouet, V., & Moore, D. J. P. (2018). Relative influences of multiple sources of uncertainty on cumulative and incremental tree-ring-derived aboveground biomass estimates. Trees, 32(1), 265-276. doi:10.1007/s00468-017-1629-0

Web link: https://link.springer.com/article/10.1007%2Fs00468-017-1629-0

This project has received funding from the European Union's Horizon 2020 research and innovation programme under grant agreement No 640176

Relative influences of multiple sources of uncertainty on cumulative and incremental tree-ring-derived aboveground biomass estimates

M. Ross Alexander[1,2] · Christine R. Rollinson[3] · Flurin Babst[1,4,5] · Valerie Trouet[1] · David J. P. Moore[2]

Abstract How forest growth responds to climate change will impact the global carbon cycle. The sensitivity of tree growth and thus forest productivity to climate can be inferred from tree-ring increments, but individual tree responses may differ from the overall forest response. Tree-ring data have also been used to estimate interannual variability in aboveground biomass, but a shortage of robust uncertainty estimates often limits comparisons with other measurements of the carbon cycle across variable ecological settings. Here we identify and quantify four important sources of uncertainty that affect tree-ring-based aboveground biomass estimates: subsampling, allometry, forest density (sampling), and mortality. In addition, we investigate whether transforming rings widths into biomass affects the underlying growth-climate relationships at two coniferous forests located in the Valles Caldera in northern New Mexico. Allometric and mortality sources of uncertainty contributed most (34–57 and 24–42%, respectively) and subsampling uncertainty least (7–8%) to the total uncertainty for cumulative biomass estimates. Subsampling uncertainty, however, was the largest source of uncertainty for year-to-year variations in biomass estimates, and its large contribution indicates that between-tree growth variability remains influential to changes in year-to-year biomass estimates for a stand. The effect of the large contribution of the subsampling uncertainty is reflected by the different climate responses of large and small trees. Yet, the average influence of climate on tree growth persisted through the biomass transformation, and the biomass growth-climate relationship is comparable to that found in traditional climate reconstruction-oriented tree-ring chronologies. Including the uncertainties in estimates of aboveground biomass will aid comparisons of biomass increment across disparate forests, as well as further the use of these data in vegetation modeling frameworks.

Keywords Carbon cycle · Aboveground biomass estimates · Uncertainty · Tree rings · Growth-climate relationships

Introduction

Whether the biosphere will act as a source or sink of carbon in the next century depends, in part, on how forest ecosystems respond to changing climate conditions (Friedlingstein et al. 2006). Forests account for 30% of the terrestrial land area and store almost 45% of the terrestrial carbon (Bonan 2008). Evaluation of the sensitivity of carbon uptake to climate, however, is challenging. Direct manipulations of temperature and rainfall are typically limited to small stature

ecosystems and short time scales (Shaver et al. 2000; Lu et al. 2012). In established forest ecosystems, we are limited to estimating carbon uptake in response to current or historical climate using methods such as forest inventories, eddy-covariance towers, or remote sensing. Estimates of forest carbon uptake from these sources are thus an important benchmark for land surface models (Beer et al. 2010). However, these datasets are only available for a fraction of the lifespan of trees, and the variance in temperature and rainfall recorded in these relatively short-term records are typically a poor sample of long-term oscillations in the climate system. Furthermore, harmonized continental- or global-scale products often rely on simplifying assumptions such as the use of global, non-species or site-specific allometric equations that complicate comparisons with field data.

Multi-century and even multi-millennial tree-ring chronologies detail the seasonal and annual climate variability experienced by temperate, boreal, and alpine trees over the course of their lifespan (Mann et al. 1998; Cook et al. 2004; Griffin et al. 2011; Williams et al. 2013; Belmecheri et al. 2015). For example, winter precipitation and summer temperature are the most influential growth factors for trees in semi-arid regions (Touchan et al. 2011; Brice et al. 2013, St. George and; Ault 2014, St. George 2014) whereas forests in more mesic environments are most strongly influenced by summer precipitation (St. George et al. 2010, St. George 2014). Furthermore, tree-ring data have been useful in developing stand-level biomass reconstructions to investigate long-term trends in aboveground productivity, and specifically the interannual fluctuations of this large carbon pool as a result of changing environmental conditions (Graumlich et al. 1989, Babst et al. 2014a, b; Dye et al. 2016).

There are, however, several limitations to using tree-ring records to infer climate sensitivities of carbon uptake. In most tree-ring analyses, the mean ring-width increment across multiple individuals is used to represent the growth at the site level (Hughes et al. 2011). However, this method can ignore the individual tree-level variability that is ecologically-relevant and contributes to the stand-level growth response in each year. Factors such as tree size, competition, topography, and microclimate can cause different annual responses among individuals and may not be captured by sampling only the largest and oldest individuals at a site, as is common in many dendrochronological studies (Esper et al. 2008; Carnwath et al. 2012; Nehrbass-Ahles et al. 2014; Foster et al. 2016; Lenoir et al. 2017; Kovács et al. 2017). Furthermore, increment cores are records of diameter growth and must be translated to carbon uptake through the use of derived allometric equations that translate linear growth to increments of stem volume and carbon content (Graumlich et al. 1989; Jenkins et al. 2004, Babst et al. 2014a, b; Nehrbass-Ahles et al. 2014). Stand density can also affect biomass estimates. Traditional dendroclimatology sampling methods greatly overestimate the potential biomass on the landscape by only sampling the oldest or largest individuals (Nehrbass-Ahles et al. 2014). Not only does this potentially overestimate the biomass estimates, but it may also influence our quantifications of how climate influences tree growth (Nehrbass-Ahles et al. 2014). Therefore, ecological sampling designs where all individuals in a fixed plot or a random sub-sample are included have been implemented to estimate forest productivity (e.g. Davis et al. 2009, Babst et al. 2014b; Dye et al. 2016). Finally, trees that are on the landscape today do not necessarily represent all trees that have contributed to biomass increment in the past. This uncertainty increases as one goes further back in time, when less stand information is available (Swetnam et al. 1999, Babst et al. 2014a; Nehrbass-Ahles et al. 2014). However, this fading record and mortality estimates can be estimated using repeat censuses, but extended, multi-decadal census datasets are rare (Biondi 1999; van Mantgem et al. 2009; Dye et al. 2016).

Without a proper accounting of these various sources of uncertainty surrounding biomass estimates, the applicability of tree-ring data to data assimilation and vegetation modeling efforts is restricted (Keenan et al. 2011). Ecosystem models are used to forecast how forests will respond to future global changes and rely on empirical observations of biomass change for benchmarking and structural improvements (Richardson et al. 2010). Here, we aim to evaluate the climate sensitivity of tree growth and aboveground biomass increment in a semiarid forest in the Southwest USA while accounting for uncertainty in the biomass estimates. Forests in semi-arid regions are particularly sensitive to climate change, with small changes in climate and growing conditions potentially resulting in large variability in carbon uptake (Poulter et al. 2014; Ahlström et al. 2015). We estimate the uncertainty in tree-ring-based estimates of living aboveground biomass increment for two semi-arid forests from 1980 to 2011 contributed by (1) the selection of allometric equations (allometric uncertainty), (2) ability of sampled trees to capture variability and patterns in annual growth increments of the forest (subsampling uncertainty), (3) ability of sampling location to accurately capture overall mean forest density (sampling uncertainty), and (4) trends in tree mortality through time (mortality uncertainty). We then assess whether biomass transformations significantly alter the growth-climate relationship from that expressed by tree-ring chronologies.

Methods

Sampling design and site description

Two sites were sampled in the Valles Caldera National Preserve, one upper elevation and one lower elevation site, located in the Jemez Mountains of northern New Mexico.

This semi-arid continental region experiences dry conditions in May and June and frequent pulses of monsoon moisture in July and August (Coop and Givnish 2007). The upper elevation site (Upper Site; 35.89N, 106.53W) has an elevation of 3049 m.a.s.l. and is composed of 97% Engelmann spruce (*Picea engelmanii* Parry ex Engelm.; PIEN) with the scattered Douglas fir (*Pseudotsuga menziesii* (Mirb.); PSME; Anderson-Teixeira et al. 2011). The Upper Site has a mean annual temperature of 3.1 °C and a mean precipitation of 667 mm $year^{-1}$ (Anderson-Teixeira et al. 2011). The lower elevation site (Lower Site; 35.86N, 106.60W) is located at 2486 m.a.s.l., and is dominated by ponderosa pine (*Pinus ponderosa* Douglas ex C. Lawson; PIPO), with one *Populus tremuloides* Michx. individual. The mean annual temperature at the Lower Site is 6.3 °C and it receives on average 550 mm of precipitation annually (Anderson-Teixeira et al. 2011).

Previous, independent studies have generated aboveground biomass estimates for the Valles Caldera, but did not fully account for the different sources of uncertainty (Anderson-Teixeira et al. 2011). Although our research is performed at the same site, we did not replicate previously sampled locations and used a different sampling method. We established two plots of 576 m^2 at the Upper Site and one 576 m^2 and one 624 m^2 at the Lower Site. The second plot at the Lower Site was slightly larger to allow a similar number of stems to be sampled in both plots. In each plot, we counted stems greater than 6 cm in diameter and calculated stem densities of 1900 and 1100 stems ha^{-1} at the Upper Site and 1500 stems ha^{-1} and 900 stems ha^{-1} at the Lower Site.

To reconstruct living biomass (hereafter referred to as biomass), two increment cores (180° from one another) were collected from a haphazard subsample of approximately 50 trees greater than 6 cm diameter at breast height (1.4 m above the ground; DBH; Supplemental Fig. 1) within each plot (Babst et al. 2014b). A total of 201 trees were sampled across the four plots (100 trees at Lower Site; 101 trees at Upper Site; Table S1). Increment cores were mounted, sanded, and analyzed using established dendrochronology techniques (Stokes and Smiley 1968; Speer 2010). We used a combination of skeleton plotting (Douglass 1941; Stokes and Smiley 1968) and the list method (Yamaguchi 2011) to crossdate (i.e. assign precise dates to individual tree rings). Ring-width increments were then measured to the nearest 0.001 mm and the assigned dates were validated using the program COFECHA (Holmes 1983; Grissino-Mayer 2001).

The oldest sampled trees at all four plots were less than 100 years old (Table S2). At the Upper Site, 76% of the trees were successfully crossdated (Table S1), resulting in a chronology composed of 77 trees with an interseries correlation of 0.708 and an EPS of 0.961 (Table S2). Less than 3% of the trees at the Upper Site were not considered effectively dated, either visually or statistically, and 21% of the samples were unable to be analyzed due to complications during sample extraction (Table S1). Cores from the upper site were often rotten, preventing a full dendrochronological analysis. Of the trees collected at the Lower Site, 86% were crossdated, leaving 11% that did not effectively crossdate, and only 3% unable to be analyzed (Table S1). The chronology from this Lower Site was composed of 86 crossdated trees with an interseries correlation of 0.755 and an EPS of 0.975 (Table S2).

We found signs of fire or insect damage at the time of sampling (i.e. large amounts of coarse woody debris) and detected no significant growth release events in the period 1980–2011 (Supplemental Fig. 2) or in records of management practices (Touchan et al. 1996; Anschueta and Merlan 2007; Allen et al. 2008). Low intensity fire events precipitously decreased after 1900 in this area and no evidence of a large fire event was present at the time of sampling at either site (Touchan et al. 1996; Allen et al. 2008). However, as with other proxy-based reconstructions, the 'fading record' can increasingly affect the accuracy of our biomass estimates back in time, as trees that were historically present at the sites may not have been present at the time of sampling and therefore could not be sampled (Swetnam et al. 1999, Babst et al. 2014a; Nehrbass-Ahles et al. 2014). We have taken two measures to account for this: (1) we have truncated the biomass reconstruction and analysis period at 1980, as this is the period of relatively little disturbance at these sites, and (2) we use reported broad-scale mortality rates for a comparable region in the western United States (van Mantgem et al. 2009; see "Mortality Uncertainty" section below).

DBH reconstruction and gap-filling techniques

For each individual tree, annual DBH was reconstructed by subtracting ring-width increments from the DBH measured in the field in June 2011 (Davis et al. 2009; Dye et al. 2016) and then truncated at 1980 for analysis. Eccentricity in growth increment around the bole can be a confounding factor in DBH reconstructions, but a proportional method (Bakker 2005) resulted in minimal differences between the two techniques for our study period ($r^2 = 0.99$, Supplemental Fig. 3). Minimal shrinkage due to drying is likely to occur, but was assumed negligible for this study (Cole 1977). For the DBH reconstruction, individual cores from the same tree were averaged. Cores that did not statistically crossdate were still used to estimate biomass after being visually checked for dating accuracy. These cores were not used to develop the tree-ring chronologies but were included in the mean biomass estimates. To reduce the potential size bias in the biomass estimate due to the high percentage of missing trees (25 trees at the Upper Site; 13 trees at the Lower Site; Table S1; Supplemental Fig. 4), we gap-filled the missing cores for which we have DBH measurements, but no ring

widths using a generalized additive mixed model and the R package mgcv (Yee and Mitchell 1991; Wood 2004, 2011). This model fit ring width (RW) as a function of fixed, interactive effects of species (SPECIES) and DBH at time of sampling (DBH) plus an additive a cubic smoothing spline through time for tree: s($YEAR_{tree}$) (Eq. 1). Nested random effects of site, plot, and were also included. Gapfilling and all data analyses were performed using the R programming language (v. 3.2.1, R Core Team 2015).

$$RW_{YEAR,TREE} = s(YEAR_{TREE}) + SPECIES \times DBH. \quad (1)$$

Allometric uncertainty

Tree-level DBH reconstructions are transformed into biomass quantities through the use of allometric equations. As is common for most forests, no site-specific equations existed for most of our species, so we relied upon the allometric equations curated by Jenkins et al. (2004) and Chojnacky et al. (2013) for total aboveground biomass allometric equations (Component 2; Jenkins et al. 2004). Our aim was to produce biomass estimates that reflect the upper limit of uncertainty possible, and we acknowledge that using site and species-specific equations based on expert opinion may produce more accurate and precise biomass estimates. We used all available equations meeting the component and species criteria of our sample (Table S3). Species-level equations were used for PSME, POTR, and PIPO. There are not any aboveground biomass equations listed for *Pinus ponderosa* in the Jenkins database. Therefore, we used A species-level PIPO equation was produced from a reanalysis of the Jenkins et al. (2004) database (Chojnacky et al. 2013). Genus-level *Picea* equations from Jenkins et al. (2004) were used for PIEN because two total aboveground biomass equations were available. References for all equations used can be found in Supplemental Table 3.

We calculated allometric uncertainty using the 'allometry' package within the Predictive Ecosystem Analyzer (PEcAn, LeBauer et al. 2013, http://www.pecanproject.org). This package uses a Bayesian framework to combine multiple allometric relationships from Jenkins et al. (2004) into a single equation with corresponding parameter uncertainties. Using the PEcAn module, we simulated a distribution of 10,000 allometric equations for each taxa, preserving covariance among parameters and sampled from the last 5000 equations to allow for Markov chain Monte Carlo (MCMC) convergence. We randomly pulled 500 equations for each tree from the distribution for each species and used those to calculate tree-level biomass. To preserve the allometric uncertainty at the tree level while scaling up to the site level, we averaged across all individuals at the site, randomly selecting a single biomass estimate for each tree. This resulted in 500 estimates of biomass for each site. Allometric uncertainty was then described as the 95% confidence interval around the mean-centered distribution of cumulative biomass estimates.

Subsampling uncertainty

Because tree rings and biomass estimates came from a subsample of 50 trees from each plot, our biomass calculations used the mean tree growth at the site level to characterize changes in biomass through time at the stand level. This allowed us to not only present a mean estimate for biomass change, but also quantify the uncertainty present in forest-level biomass accumulation arising through the variability in individual tree growth. This approach relies on the assumption that our haphazard sample of 50 trees accurately represents the size and species distribution of all individuals in the plot. To calculate the subsampling uncertainty, we first calculated annual biomass increment for each tree using a first-difference approach and mean-centered the increment distribution. We describe the subsampling uncertainty using the 95% confidence interval around this observed distribution of values. We used both dated and gap-filled trees for this calculation, as it protects against a potential size bias of using only dated trees (Supplemental Fig. 4).

Sampling uncertainty

Sampling multiple locations in a site is the most common method of providing uncertainty in field-based biomass estimates. This uncertainty arises from spatial heterogeneity resulting in variable densities among plots. We characterized this location-based sampling uncertainty in forest density as the mean biomass for a tree at each site (kg per tree; averaged across both plots) times the density for each plot (trees per m^2). To robustly characterize sampling uncertainty, ideally all individuals in a plot would be sampled, summed to the plot level, and then that total could be averaged across more than two plots, but this was not possible in our study. Thus, we describe the uncertainty in biomass estimates from sampling uncertainty in our study as the range based on the densities observed in our two plots.

Mortality uncertainty

Long-term census data were not available for our study sites and therefore we have no records of how the loss of individuals to mortality affects biomass reconstructions at our site. Therefore, to account for the mortality-based biomass losses through time, we used regional mortality estimates from van Mantgem et al. (2009) to simulate background mortality processes and adjust the stand density applied to per-tree biomass estimates through time. van Mantgem et al. (2009) reported a baseline mortality rate in 1979 of $0.4843 \pm 0.0941\%$ $year^{-1}$ (mean ± SE) with an

annual increase in that rate of $0.024 \pm 0.027\%$ year^{-1}. We calculated mortality uncertainty in our biomass estimates by using these reported values and error estimates to generate a distribution of modifications to our initial stem densities in time. To do this, we assumed the values presented by van Mantgem et al. were normally distributed and converted standard error to standard deviation using the reported $n = 9$. We simulated a normal distribution of baseline mortality rates for 1979 that then compounded and increased in time to the present. Thus, the mortality rate in year t starting in 1980 can be described as the percent mortality rate (Mortality) in the previous year with in 1979 (normal, $\mu = 0.4843$, $\sigma = 0.2823$) plus a fractional increase in that mortality rate (Eq. 2, van Mantgem et al. 2009). The annual increase in mortality rate is described as a normal distribution (normal, $\mu = 0.024$, $\sigma = 0.081$) times the previous year's mortality rate. Density in each year can then be simulated from the present into the past as a function of the initial density in time ($t + 1$) plus the percentage of stems lost to mortality in that year (Eq. 3).

$$\text{Mortality}_t = \text{Mortality}_{t-1} + \text{Mortality}_{t-1} \times \text{Increase}, \quad (2)$$

$$\text{Density}_t = \text{Density}_{t+1} + \text{Density}_{t+1} \times \text{Mortiality}_t. \quad (3)$$

Using the errors reported by van Mantgem et al. (2009), we simulated 500 possible mortality-adjusted year-specific densities that were then multiplied with per-tree estimates of biomass. Negative simulated values that would represent recruitment were discarded in this process so that mortality would increase biomass estimates. Mortality uncertainty is described as the 95% confidence interval in the difference between biomass estimates using mortality-adjusted density relative to a static plot density using the stem density values observed in 2011.

Total uncertainty calculation

For both the cumulative and the interannual biomass reconstructions, the total uncertainty was calculated by first calculating the deviation of the upper and lower 95% confidence interval bound from the mean baseline biomass estimate: mean tree biomass estimate times mean plot density for each area of uncertainty. The upper and lower bounds for each area were then added in quadrature to quantify the total uncertainty in field-based biomass estimates. The percent contribution of each component was calculated as the component divided by the sum of all sources of uncertainty.

Climate response analyses

We assessed the response of tree growth and above ground biomass increment to interannual variability in precipitation and temperature through a series of Pearson correlation analyses. We compared the growth-climate relationships of four tree-ring width chronologies to that of the mean annual biomass increment (BM) time series per site. Three tree-ring chronologies were calculated per site from our samples using (1) all crossdated trees, (2) the largest 10% of crossdated trees, and (3) the smallest 10% of crossdated trees (hereafter referred to as All, Large, and Small, respectively). At the Upper and Lower Sites, respectively, the All chronologies represent diameter ranges of 6.8–53.6 and 10.2–40.5 cm, the Small chronologies are composed of diameters ranging from 6.8 to 10.0 cm ($n = 11$) at the Upper Site and 10.2–13.1 cm ($n = 10$) at the Lower Site. The Large chronologies are composed of diameters from 34.8 to 53.6 cm ($n = 11$) at the Upper Site and 34.5–40.5 cm ($n = 10$) at the Lower Site. We obtained additional tree-ring width chronologies that were specifically sampled for dendroclimatic purposes ('ITRDB') at Valles Caldera from the International Tree-Ring Data Bank that were built from similar species at similar elevations. We used the chronology developed by Touchan et al. (PSME; 2011) and Brice et al. (PIPO; 2013) to evaluate the growth-climate responses at the Upper Site and Lower Site, respectively. Each chronology was generated using a 30-year cubic smoothing spline to detrend individual series and the biweight robust mean was calculated to create a site level chronology (Cook 1985; Cook and Peters 1997). The BM time series was not detrended, because detrended data would not be used in land-surface model data assimilation, and detrending had little effect on the overall growth-climate response (Supplemental Fig. 5). We compared the BM time series and tree-ring width chronologies to PRISM temperature and precipitation data (PRISM Climate Group 2004). We extracted climate data for each of our sampled sites and aggregated to the following seasons: previous fall (pFall) = pSept, pOct, pNov; Winter = pDec, Jan, Feb; Spring = Mar, Apr, May; Summer = June, July, Aug. We then used a Pearson's correlation analysis on the common overlapping period of all time series (1980–2007) to determine significant climate correlations with statistical significance defined as $p < 0.05$.

To determine how the full range of uncertainties might affect the biomass growth-climate relationship, we bootstrapped 30,000 independent, random draws with replacement from the observed distribution of each area of uncertainty: allometry, sub-sampling, sampling, and mortality. 500 values from each source of uncertainty were independently drawn and added together in quadrature to generate 30,000 simulated BM time series. We then performed a similar correlation analysis as described above to assess the uncertainty in growth-climate relationships of the series. We assessed the differences in climate response from the biomass increment responses of (1) all trees, (2) the largest 10% of trees, (3) the smallest 10% of trees at each site. The size categories were based off the same DBH ranges as

stated above for the tree-ring width chronologies. We identified relationships as significant if the 95% CI of the critical values did not encompass zero.

Results

The relative contribution of sources of uncertainty differed between cumulative biomass estimates and interannual biomass estimates. The mean cumulative biomass at the time of sampling at the Lower Site (PIPO) was 20.95 kg m^{-2}, with a lower 95% CI of 18.54 kg m^{-2} and an upper 95% CI of 23.54 kg m^{-2}, and the mean biomass of the Upper Site (PSME/PIEN) was 24.47 kg m^{-2}, with a lower 95% CI of 16.96 kg m^{-2} and an upper 95% CI of 35.19 kg m^{-2} (Fig. 1). With the exception of the allometric uncertainty, the ranges of uncertainty are comparable across both sites (Table 1). At the Upper Site, allometric and mortality components account for over 75% of the total uncertainty in cumulative biomass, with uncertainty in the allometric equations accounting for 58 ± 9% (mean ± SD; 1980–2011) and mortality accounting for 24 ± 11% from 1980 to 2011 (Fig. 2; Table 1). At the Lower Site, allometric uncertainty accounts for 34 ± 11% and mortality accounts for 42 ± 16% of the total uncertainty in cumulative biomass. The subsampling uncertainty contributed the least to the overall cumulative biomass uncertainty at the upper and Lower Sites (7 ± 2 and 8 ± 3%, respectively; Fig. 2; Table 1).

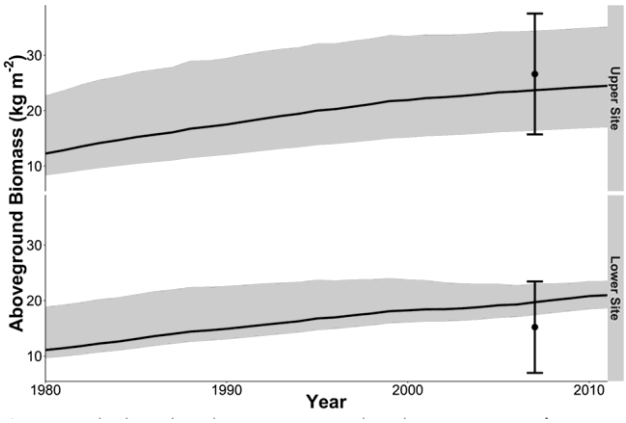

Fig. 1 Site-level cumulative biomass estimates with total uncertainty ranges for an upper elevation Engelmann spruce dominated (Upper Site) and lower elevation ponderosa pine dominated forest (Lower Site) at the Valles Caldera, NM. The dark black line represents the mean cumulative biomass estimate traditionally reported, and the shaded grey area is the 95% CI of biomass from adding all sources of uncertainty together in quadrature. Points and error bars represent an independent assessment (mean ± 1.96*SD; $n = 4$) of living biomass (assuming a 50% carbon content) from 2007 for both sites (Anderson-Teixeira et al. 2011)

Table 1 mean ± SD for cumulative and incremental living aboveground biomass uncertainty ranges (kg m^{-2}) for 1980–2011 of major sources of variability at an upper elevation and a lower elevation forest in the Valles Caldera, NM

Source	Cumulative range (kg BM m^{-2})		Incremental range (kg BM m^{-2} $year^{-1}$)	
	Upper site	Lower site	Upper site	Lower site
Allometric	14.88 ± 2.14	3.89 ± 0.47	0.20 ± 0.09	0.15 ± 0.06
Subsampling	1.84 ± 0.76	0.98 ± 0.30	1.84 ± 0.76	3.19 ± 1.25
Sampling	2.86 ± 1.35	1.78 ± 0.21	0.13 ± 0.07	0.85 ± 0.36
Mortality	6.39 ± 2.82	5.39 ± 2.50	0.30 ± 0.19	0.61 ± 0.40
Total	17.67 ± 0.93	8.15 ± 1.73	1.95 ± 0.70	1.06 ± 0.25

Total uncertainty is calculated by adding the upper and lower 95% confidence intervals of each area of uncertainty in quadrature

The mean interannual biomass increment at the Upper Site was 0.39 ± 0.16 kg BM m^{-2} $year^{-1}$ with an upper 95% CI of 1.88 ± 0.76 kg BM m^{-2} $year^{-1}$ and a lower 95% CI of − 0.08 ± 0.08 kg BM m^{-2} $year^{-1}$. The negative lower CI indicates the potential impact that the mortality uncertainty has on the overall biomass uncertainty from year to year. At the Lower Site the mean annual biomass increment was 0.32 ± 0.3 kg BM m^{-2} $year^{-1}$ with an upper 95% CI of 1.02 BM m^{-2} $year^{-1}$ and a lower 95% CI of − 0.04 kg BM m^{-2} $year^{-1}$. Subsampling uncertainty accounted on average for more than 70% of the interannual biomass subsampling uncertainty at both the Upper and the Lower Sites (70 ± 10 and 71 ± 14%, respectively; Fig. 3; Table 1). Second to subsampling uncertainty, mortality uncertainty accounted for 21 ± 16% of the total annual biomass subsampling uncertainty at the Lower Site and 16 ± 13% at the Upper Site (Fig. 3; Table 1). At the Lower Site, sampling uncertainty contributed the least to the overall subsampling uncertainty (3 ± 2%), whereas allometric uncertainty composed 4 ± 1% (Fig. 3). Allometric uncertainty played a larger role at the Upper Site, contributing 8 ± 2%, and sampling uncertainty contributed the least with 5 ± 2% of the overall subsampling uncertainty.

The climate sensitivities of the BM time series at both sites were similar to that expressed by the four tree-ring width time series (Fig. 4). A signal typical of the Southwestern US can be seen at both sites and across all chronologies analyzed, with negative relationships with spring and summer temperatures and positive relationships with previous fall, winter, and spring precipitation (Fig. 4). At the Upper Site, the BM time series generally reflected the signal in the All chronology and the ITRDB chronology. However, the BM time series showed a significant negative correlation with summer temperature and a significant positive correlation with summer precipitation, when neither the All chronology nor the ITRDB chronology do so (Fig. 4). The Large chronology at the Upper Site showed similar summer

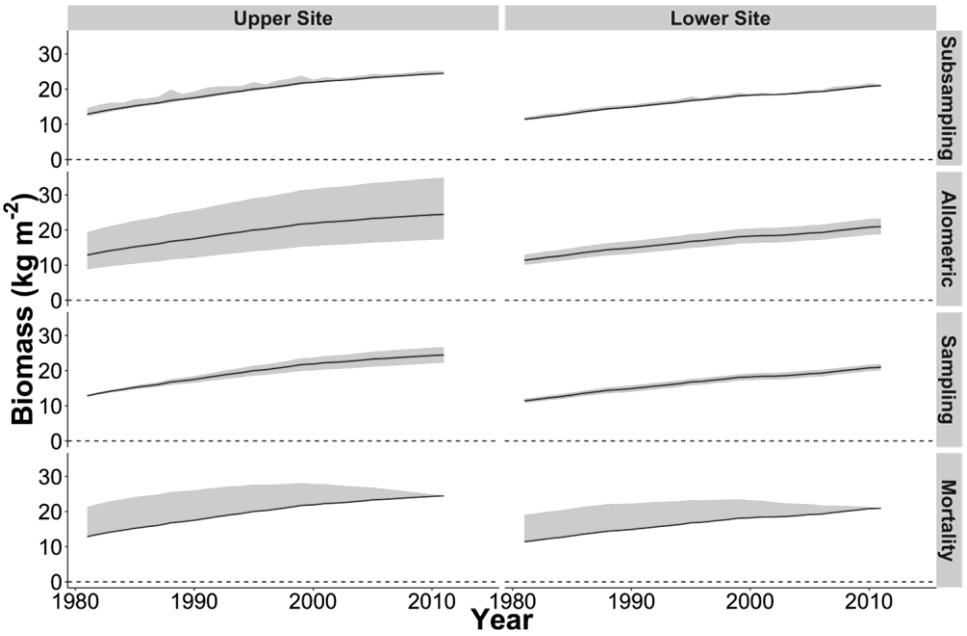

Fig. 2 Cumulative tree-ring-derived biomass estimates for the Upper Site (left column) and the Lower Site (right column) at the Valles Caldera. The black line represents the biomass calculated for the mean allometric equation for each site, and the shaded area is the 95% confidence interval for each source of uncertainty

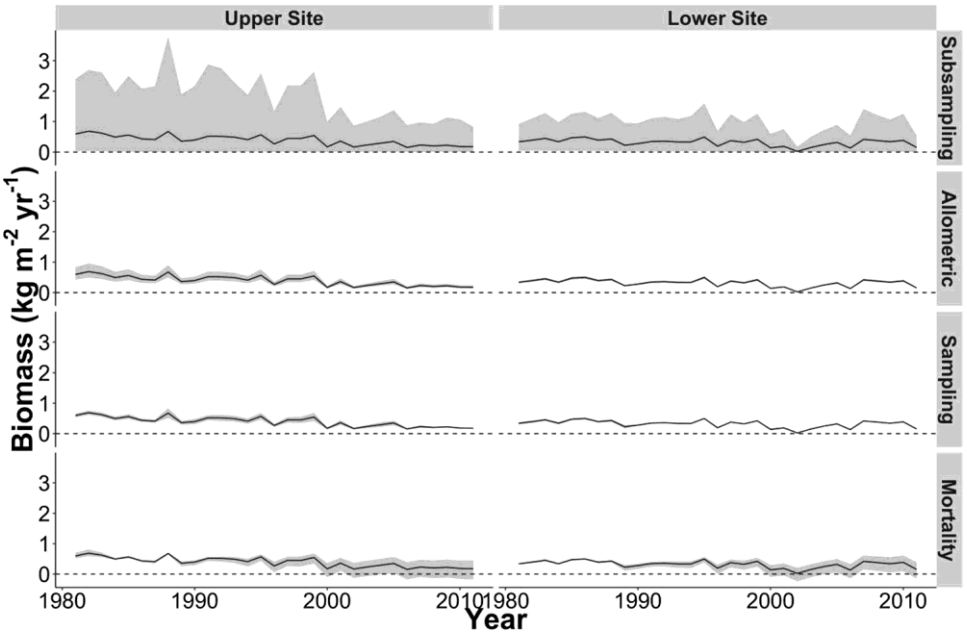

Fig. 3 Interannual tree-ring-derived biomass estimates for the Upper Site (left column) and the Lower Site (right column) at the Valles Caldera. The black line represents the mean interannual biomass increment calculated for each site, and the shaded area is the 95% confidence interval for each source of uncertainty

correlations to those of the BM time series, indicating that in the summer months the largest trees at the Upper Site are contributing more to this particular climate response (Fig. 4). The growth responses are relatively consistent between the Large chronology and the Small chronology, with notable differences in both the summer temperature and precipitation responses. In both cases, the growth response of the Large chronology was stronger than that of the Small chronology. At the Lower Site, the BM time series showed a significant negative relationship with temperature during the previous fall and the current summer, but not a significant relationship with spring temperatures. This is different than any of the tree-ring chronologies from this site, which all show a significant negative response to spring temperature (Fig. 4).

The general growth-climate relationships for the biomass increment time series using the full uncertainty distribution were similar to those for the mean BM and tree-ring chronology assessment, but illustrate the breadth of climate response upon translating tree-ring data into biomass (Figs. 4, 5). Across both sites, the smallest trees show a relatively narrow range of climate responses, compared to the largest trees

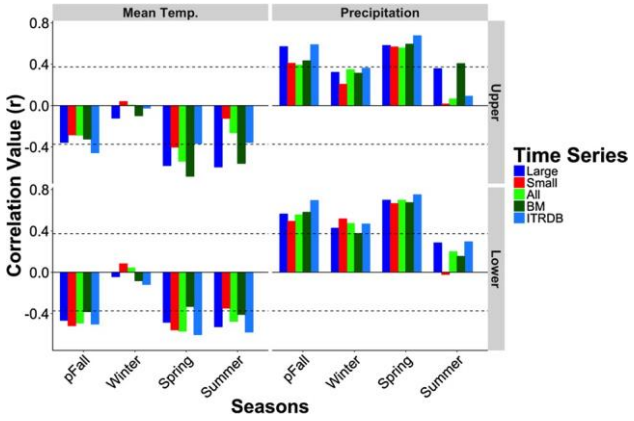

Fig. 4 Seasonal (previous Fall, Winter, Spring, Summer) growth-climate response of mean biomass increment estimates (dark green) and four tree-ring chronologies (Large, Small, All, ITRDB) with mean temperature and total precipitation at an upper (Upper Site) and a lower (Lower Site) elevation site in the Valles Caldera, NM. The Large chronology (blue) is composed of the largest 10% of trees by DBH and the Small chronology (red) is composed of the smallest 10%. The ITRDB chronology (light blue) was gathered from ITRDB (Upper Site: Touchan et al. 2011; Lower Site: Brice et al. 2013). The mean biomass increment time series (light green) represents the mean annual biomass increment for each site. Significant responses were identified as those values exceeding the ($\alpha = 0.05$) significance criterion (dashed line)

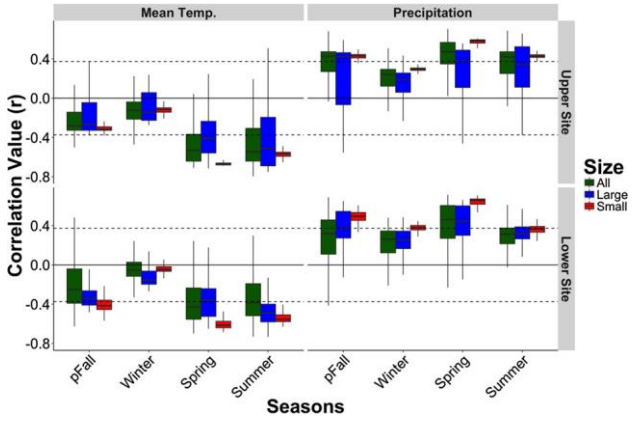

Fig. 5 Distributions of growth-climate relationships for simulated biomass time series from an upper elevation (Upper Site; PIEN) and a lower elevation (Lower Site; PIPO) forest in the Valles Caldera, NM. The Large time series is based on the largest 10% of trees, the Small time series is based on the smallest 10% of trees, and the All time series is composed of all trees sampled. Distributions were generated by bootstrapping, with replacement, 30,000 time series meeting each of the three criteria and performing a Pearson's correlation analysis. Solid bars refer to the mean *r* value

(Fig. 5). Once transformed into biomass, the mean summer growth response of the Small trees is strengthened, whereas the mean response of the largest trees appears to be muted, likely due to the highly-varied climate response (Figs. 4, 5).

Discussion

The application of tree rings to aboveground biomass assessments provides time series of biomass change that are similar to, but more finely-resolved than estimates from periodic census data (Dye et al. 2016). However, appropriate uncertainties must be reported alongside these estimates to facilitate comparisons among disparate locations and data types. Without the accompanying uncertainties, comparisons between similar forest types can be misleading. For example, our mean estimate of total aboveground biomass at the Lower (PIPO) site was 19.7 kg BM m^{-2} in 2007. Without uncertainties or margins of error, this would appear high when compared to comparable values from similar regions and forest types. A study whose sites are proximal to our own estimated aboveground biomass at the Lower (PIPO) site to be 15.3 ± 4.2 kg BM m^{-2} (mean ± SD; Anderson-Teixeira et al. 2011, Table S2) in 2007. In other southwest PIPO forests, Kaye et al. (2005) estimated aboveground biomass has been estimated as 12.7 ± 2.2 kg BM m^{-2} in 1995, and Finkral and Evans (2008) observed a range of biomass of 5.9–14.1 ± 3.0 kg BM m^{-2}. However, when the full range of uncertainty is considered, our aboveground biomass estimate (17.3–23.0 kg BM m^{-2}; 95% CI) is consistent with these previously reported values.

We found that uncertainty due to the choice in the allometric equation is the largest contributor to the overall uncertainty in cumulative biomass estimates at our site (Fig. 2). Choice of allometric equation has substantial influence over the initial value of biomass reconstructions (Chave et al. 2004), however, this area of uncertainty is seldom reported, despite both the plethora and dearth of equations that can exist for any one species (Jenkins et al. 2004; Chojnacky et al. 2013, Supplemental Table 3). The most commonly reported uncertainty associated with biomass quantities is the variability among plots, what we term 'sampling' uncertainty. The spatial heterogeneity of biomass across the landscape can be quite large, with the 95% CI consisting of between 34 and 100% of the mean biomass estimates reported by other studies in similar forest types (Kaye et al. 2005; Finkral and Evans 2008; Anderson-Teixeira et al. 2011). The uncertainties that accompany tree-ring-derived estimates of aboveground biomass are also influenced by a combination of temporally static factors such as allometric equation choice, and temporally dynamic factors such as annual increment and mortality rate. Yet, despite the process involved in transforming tree-ring increments into estimates of aboveground biomass, the growth-climate relationships observed in our tree-ring chronologies persist (Figs. 4, 5). This means that, at least in climate-sensitive regions such as the semi-arid, American Southwest (St. George and Ault

2014), the observed growth-climate relationships will be accurately represented in the aboveground biomass estimates that are subsequently incorporated into large-scale modeling frameworks.

Not all trees in the stand respond similarly to interannual variation in climate. Subsampling uncertainty accounts for at least 70% of the total interannual biomass increment uncertainty, and arises when extrapolating the observed, individual-level growth patterns to represent that of the entire stand. However, the represented climate signal may change depending on the climate sensitivity of the species sampled and the manner in which those trees are selected (Nehrbass-Ahles et al. 2014, St. George and; Ault 2014). The crossdating process is integral to the proper quantification of this area of uncertainty to temporally align the annual growth of individual trees (Black et al. 2016). The mean growth increment is often used in dendrochronology to characterize and understand the mechanisms that affect tree growth at the site level. However, using the mean value in these analyses can overlook factors that influence tree growth, such as stand dynamics or size. For example, Nehrbass-Ahles et al. (2014) found that sampling design had little influence on the climate signal that was expressed by the standard mean tree-ring chronology, as using the mean has a stabilizing effect on the expressed climate signal. We found a similar result (Fig. 4): the growth-climate responses of the mean tree-ring width chronologies and BM time series are similar. However, we see differing strengths in the correlations with climate of Large and Small trees (Figs. 4, 5), which may indicate how asymmetric competition within the stand influences climate responses (Canham et al. 1994; Rollinson et al. 2016). The mean forest response characterizes the general growth-climate relationship of the larger, more dominant trees (Figs. 3, 4), and by presenting the subsampling uncertainty alongside the mean biomass estimate we can gain a more nuanced view of the growth-climate relationships of non-dominant forest components (Rollinson et al. 2016). Tree-ring increments cannot provide a time series of interannual changes in bark thickness. For our calculations we have assumed a constant bark thickness with a changing ring-width increment, and recognize that this may not be an accurate depiction of allocation of resources to bark through time. The subsampling uncertainty is present at both the cumulative and incremental time steps, but is a relatively minor component compared to other sources of uncertainty at the cumulative level (Fig. 2).

The choice of allometric equation strongly influences the cumulative biomass estimate (Fig. 2), but had a minimal effect on the interannual biomass increment (Fig. 3). At the Upper Site, allometric uncertainty comprised 57 ± 8% of the total uncertainty around cumulative biomass, whereas at the Lower Site it only contributed 34 ± 11% to the overall cumulative uncertainty. Chave et al. (2004) found that allometric uncertainty in tropical trees can dominate over sampling uncertainty. We also see that allometric uncertainty dominates the cumulative biomass uncertainty at our sites. However, at the incremental scale, its influence is less than that of the subsampling variability (Figs. 2, 3). Allometric equations allow for diameter reconstructions to be transformed into biomass estimates, but uncertainties exist within and among allometric equations (Chave et al. 2004; Nickless et al. 2011, Babst et al. 2014a). Large syntheses and databases (Jenkins et al. 2004; Chojnacky et al. 2013) have made allometric equations more accessible, but the variability in equations among species, size classes, and across sites (Ketterings et al. 2001) make it difficult to identify the most appropriate equation for a given study.

Ideally, any reconstruction of biomass would rely on site-specific allometric equations, but even site-specific equations will contain parameter uncertainties that should be reported to facilitate easier comparisons between sites and among equations. By using a Bayesian approach (LeBauer et al. 2013) we generated parameter-based uncertainties that included all of the equations available for each species from the Jenkins et al. (2004) database, and thus have illustrated the full range of biomass estimates possible from these equations. Using all available equations has likely increased the uncertainty in our biomass estimates. However, due to strong influences of fine-scale environmental variability and phenotypic plasticity in growth form (Weiner 2004), even locally-derived equations may not accurately represent all trees sampled in any one study (Chave et al. 2004).

Sampling uncertainty is influenced by the forest structure and the chosen sampling design. A sampling design that both accurately represents the variability among individuals within the forest, yet is feasible to implement, has always been a concern in ecological research (Botkin and Simpson 1990; Pacala et al. 1996; Mackenzie and Royle 2005). Nehrbass-Ahles et al. (2014) recently advocated for the use of 25 m fixed radius plots as a practical means to estimate aboveground biomass in European forests. However, in our least dense plot (0.09 trees m^{-2}) this would have resulted in 176 trees per plot, whereas a mean of 57 trees were present in the Nehrbass-Ahles et al. (2014) plots. The range of sampling uncertainties at the Upper and Lower sites was comparable to those reported for nearby sites within the Valles Caldera. In 2007, the living biomass at the site was reported as 26.6 ± 10.8 kg BM m^{-2} (mean ± 95% CI; assuming a 50% C content; Anderson-Teixeira et al. 2011 Table S2) and 15.2 ± 8.2 kg BM m^{-2} at the Upper and Lower sites, respectively (Fig. 1). The reported uncertainty overlaps with the full range of uncertainty observed at our sites (Fig. 1), but is larger than the range of our reported sampling uncertainty (1.35 and 0.21 kg BM m^{-2} at the Upper and Lower Sites, respectively; Anderson-Teixeira et al. 2011, Table S2). It is likely that the previous study analyzed a dataset with

greater spatial diversity, but the reported uncertainties facilitate comparisons between the two biomass estimates.

Tree-ring investigations of mortality are traditionally focused on establishing the timing of an event (Foster 1988; Swetnam and Lynch 1989; Daniels et al. 1997), but quantifying the extent of a past mortality events is highly situational (Rubino and McCarthy 2004). Our sites were relatively even-aged and no major anthropogenic or natural disturbances were recorded over the lifespan of most trees (Touchan et al. 1996; Anschueta and Merlan 2007; Allen et al. 2008; Supplemental Fig. 2), but we have limited our analysis to the period 1980–2011 to overcome the challenges associated determining a representative mortality rate. Long-term census data have been used to determine timing of individual mortality events, but these datasets are sparse and time consuming to generate (Eisen and Plotkin 2015). However, when these data are available, tree-ring estimates of aboveground biomass at the same site fall within the 95% confidence interval of the permanent plots, suggesting that, to a point, tree rings can be used to accurately depict aboveground carbon dynamics (Dye et al. 2016). We chose to use generalized mortality values from the interior western US (van Mantgem et al. 2009) to estimate changing stand densities and thus biomass load back through time, but localized mortality rates or detrital biomass loads would increase the accuracy of this source of uncertainty. We acknowledge that mortality is more episodic than is indicated by our continuous mortality rate, and often occurs as sudden die-off events (Allen et al. 2010) or gap dynamics (Pederson et al. 2014) rather than a constant self-thinning rate that we describe in this paper. These die-off events would manifest themselves in the existing tree-ring record as synchronous increases in the growth (release events) of nearby surviving trees, and thereby affecting the mortality uncertainty of the biomass reconstruction (Lorimer and Frelich 1989). There is no evidence that such an event occurred at the sites we studied from 1980 to 2011 (Supplemental Fig. 2). Mortality is a difficult process to constrain, both in the lab (Fisher et al. 2010) and in the field (Allen et al. 2010), but continued measurement efforts across diverse sites will greatly improve the accuracy of mortality estimates from isolated stands to landscape-level processes.

The climate response patterns in both our chronologies and biomass estimates adhere to what is known about forests in this region: they are strongly influenced by winter precipitation and spring temperatures, prior to the hot premonsoon summer conditions (St George et al. 2010; Touchan et al. 2011; Griffin et al. 2013, St George and Ault 2014). In general, growth-climate relationships of the BM time series are similar to that of the mean tree-ring chronology based on all trees, with the exception of the increased summer precipitation response (Fig. 4). Detrending the biomass data did little to change the growth-climate relationship (Supplemental Fig. 5). The effect of the large contribution of the incremental upscaling uncertainty (Fig. 3) can be seen in the different climate responses of large and small trees (Fig. 4). Using only the growth-climate response of the largest trees does change the observed pattern at both sites (Figs. 3, 4). On a per-stem basis, large trees disproportionately contribute more to the total forest biomass estimate than smaller trees. Therefore, it is not unreasonable that the growth signal of the largest trees most closely resembles the forest-level response (Lutz et al. 2012; Slik et al. 2013). The differences between responses of Large and Small trees could indicate the impacts asymmetric competition or access to water sources may have on climate response (Rollinson et al. 2016; Kerhoulas et al. 2013). Both forests had relatively simple canopy structures, but the broad response of the Large trees suggests that they are still experiencing varied environmental and ecological conditions that affects their sensitivity to climate (Carnwath et al. 2012).

Accurately projecting future changes to the terrestrial carbon cycle depend in part on characterizing the long-term response of ecosystems to climate (Friedlingstein et al. 2006). To this end, tree rings are useful in estimating aboveground biomass for various forest ecosystems over longer time periods (Graumlich et al. 1989, Babst et al. 2014a, b; Nehrbass-Ahles et al. 2014; Dye et al. 2016), but we must continue to develop this technique to better understand the terrestrial carbon cycle. Individual trees compose the forest and it is the growth response of these individuals that affects the concerted ecosystem response. As tree rings are increasingly used in studies of carbon dynamics (Babst et al. 2014a; Nehrbass-Ahles et al. 2014; Dye et al. 2016), the methods must continue adapt to understand the growth-climate relationships at multiple scales. In the case of terrestrial carbon and biomass studies, our study suggests that both climate and ecological variables such as stand density and competition have strong effects on tree growth and that the ecosystem response to climate can be more variable than what is represented by a subsample trees in a particular age or size class. Tree rings provide a means to generate both cumulative and interannual increment estimates of aboveground biomass, but the lack of uncertainty estimates limits the inferences and comparisons that can be made (Keenan et al. 2011). Uncertainty estimates will facilitate the creation of large-scale biomass networks, providing an empirical basis from which to model carbon cycle dynamics.

Acknowledgements This research was supported by the DOE Regional and Global Climate Modeling program DE-SC0016011 and by the University of Arizona Water, Environment, and Energy Solutions (WEES) and Sustainability of Semi-Arid Hydrology and Riparian Areas (SAHRA) programs. FB acknowledges funding from the Swiss National Science Foundation (Grant #P300P2_154543) and the EU H2020 Program (Grant 640176, "BACI"). The authors would like to thank Emily Dynes, Ian Schiach, and Bhaskar Mitra for help with

sample collection, Amy Hudson for statistical input, and Marcy Litvak for her helpful comments and insights into the Valles Caldera.

Author contributions MRA, VT, and DJPM conceived of main analyses and conducted field sampling. MRA performed tree ring analysis and data generation. MRA and CRR contributed to code generation and uncertainty analyses. All authors contributed to intellectual project development and to manuscript preparation and writing.

Compliance with ethical standards

Conflict of interest The authors declare that they have no conflicts of interest.

References

Ahlström A, Raupach MR, Schurgers G et al (2015) The dominant role of semi-arid ecosystems in the trend and variability of the land CO_2 sink. Science 348:895–899

Allen CD, Anderson RS, Jass RB, Toney JL (2008) Paired charcoal and tree-ring records of high-frequency Holocene fire from two New Mexico bog sites. Int J Wildland Fire 17:115–130

Allen CD, Macalady AK, Chenchouni H et al (2010) A global overview of drought and heat-induced tree mortality reveals emerging climate change risks for forests. For Ecol Manage 259:660–684

Anderson-Teixeira KJ, Delong JP, Fox AM et al (2011) Differential responses of production and respiration to temperature and moisture drive the carbon balance across a climatic gradient in New Mexico. Global Change Biol 17:410–424

Anschueta KF, Merlan T (2007) More than a scenic mountain landscape: Valles Caldera National Preserve land use history. Forest Service Rocky Mountain Research Station Gen. Tech. Rep. RMRSGTR-196. Fort Collins, CO

Babst F, Alexander MR, Szejner P et al (2014a) A tree-ring perspective on the terrestrial carbon cycle. Oecologia 176:307–322

Babst F, Bouriaud O, Alexander R et al (2014b) Toward consistent measurements of carbon accumulation: a multi-site assessment of biomass and basal area increment across europe. 32:153–161

Bakker JD (2005) A new, proportional method for reconstructing historical tree diameters. Can J For Res 35:2515–2520

Beer C, Reichstein M, Tomelleri E et al (2010) Terrestrial gross carbon dioxide uptake: global distribution and covariation with climate. Science 329:834–838

Belmecheri S, Babst F, Wahl ER et al (2015) Multi-century evaluation of Sierra Nevada snowpack. Nat Clim Change 6:2–3

Biondi F (1999) Comparing tree-ring chronologies and repeated timber inventories as forest monitoring tools. Ecol Appl 9:216–227

Black BA, Griffin D, van der Sleen P et al (2016) The value of crossdating to retain high-frequency variability, climate signals, and extreme events in environmental proxies. Global Change 22:2582–2595

Bonan GB (2008) Forests and climate change: forcings, feedbacks, and the climate benefits of forests. Science 320:1444–1449

Botkin DB, Simpson LG (1990) Biomass of the North American boreal forest: a step toward accurate global measures. Biogeochemistry 9:161–174

Brice B, Lorion KK, Griffin D et al (2013) Signal strength in subannual tree-ring chronologies from pinus ponderosa in northern New Mexico. Tree Ring Res 69:81–86

Canham CD, Finzi AC, Pacala SW, Burbank DH (1994) Causes and consequences of resource heterogeneity in forests—interspecific variation in light transmission by canopy trees. Can J For Res 24:337–349

Carnwath GC, Peterson DW, Nelson CR (2012) Effect of crown class and habitat type on climate–growth relationships of ponderosa pine and Douglas-fir. For Ecol Manage 285:44–52

Chave J, Condit R, Aguilar S et al (2004) Error propagation and scaling for tropical forest biomass estimates. Philos Trans R Soc Lond B Biol Sci 359:409–420

Chojnacky DC, Heath LS, Jenkins JC (2013) Updated generalized biomass equations for North American tree species. Forestry 87:129–151

Cole DM (1977) Protecting and storing increment cores in plastic straws. USDA Forest Service Intermountain Forest and Range Experiment Station Research Note INT-216. Ogden, UT

Cook ER (1985) A time series analysis approach to tree ring standardization. PhD dissertation, University of Arizona, Tucson, p 175

Cook ER, Peters K (1997) Calculating unbiased tree-ring indices for the study of climatic and environmental change. Holocene 7:361–370

Cook ER, Woodhouse CA, Eakin CM et al (2004) Long-term aridity changes in the western United States. Science 306:1015–1018

Coop JD, Givnish TJ (2007) Spatial and temporal patterns of recent forest encroachment in montane grasslands of the Valles Caldera, New Mexico, USA. J Biogeogr 34:914–927

Daniels LD, Dobry J, Klinka K, Feller MC (1997) Determining year of death of logs and snags of *Thuja plicata* in southwestern coastal British Columbia. Can J For Res 27:1132–1141

Davis SC, Hessl AE, Scott CJ, Adams MB (2009) Forest carbon sequestration changes in response to timber harvest. Forest Ecol 258:2101–2109

Douglass AE (1941) Crossdating in dendrochronology. J For 39:825–831

Dye A, Barker Plotkin A, Bishop D et al (2016) Comparing tree-ring and permanent plot estimates of aboveground net primary production in three eastern U.S. forests. Ecosphere 7:1–13

Eisen K, Plotkin AB (2015) Forty years of forest measurements support steadily increasing aboveground biomass in a maturing, Quercus-dominant northeastern forest. J Torrey Bot Soc 142:97–112

Esper J, Niederer R, Bebi P, Frank D (2008) Climate signal age effects—evidence from young and old trees in the Swiss Engadin. For Ecol Manage 255:3783–3789

Finkral AJ, Evans AM (2008) The effects of a thinning treatment on carbon stocks in a northern Arizona ponderosa pine forest. For Ecol Manage 255:2743–2750

Fisher R, McDowell N, Purves D et al (2010) Assessing uncertainties in a second-generation dynamic vegetation model caused by ecological scale limitations. New Phytol 187:666–681

Foster DR (1988) Disturbance History, Community Organization and Vegetation Dynamics of the Old-Growth Pisgah Forest., South-Western New Hampshire. J Ecol 76:105–134

Foster JR, Finley AO, D'Amato AW et al (2016) Predicting tree biomass growth in the temperate–boreal ecotone: is tree size, age, competition, or climate response most important? Glob Change Biol 2138–2151

Friedlingstein P, Cox P, Betts R et al (2006) Climate-carbon cycle feedback analysis: results from the C4MIP model intercomparison. J Geophys Res Biogeosci 19:3337–3353

Graumlich LJ, Brubaker LB, Grier CC (1989) Long-term trends in forest net primary productivity: Cascade Mountains, Washington. Ecology 70:405

Griffin D, Meko DM, Touchan R et al (2011) Latewood chronology development for summer-moisture reconstruction in the US Southwest. Tree Ring Res 67:87–101

Griffin D, Woodhouse CA, Meko DM et al (2013) North American monsoon precipitation reconstructed from tree-ring latewood. Geophys Res Lett 40:954–958

Grissino-Mayer HD (2001) Evaluating crossdating accuracy: a manual and tutorial for the computer program COFECHA. Tree Ring Res 57:205–221
Holmes RL (1983) Computer-assisted quality control in tree-ring dating and measurement. Tree Ring Bull 43:69–78
Hughes MK, Diaz HF, Swetnam TW (2011) Tree rings and climate: sharpening the focus. In: Hughes MK, Swetnam TW, Diaz HF (eds) Dendroclimatology. Springer, Netherlands, Dordrecht, pp 331–353
Jenkins JC, Chojnacky DC, Heath LS, Birdsey RA (2004) Comprehensive database of diameter-based biomass regressions for North American tree species. US Department of Agriculture, Forest Service, Newtown Square, PA
Kaye JP, Hart SC, Fulé PZ et al (2005) Initial carbon, nitrogen, and phosphorus fluxes following ponderosa pine restoration treatments. Ecol Lett 15:1581–1593
Keenan TF, Carbone MS, Reichstein M, Richardson AD (2011) The model–data fusion pitfall: assuming certainty in an uncertain world. Oecologia 167:587–597
Kerhoulas LP, Kolb TE, Koch GW (2013) Tree size, stand density, and the source of water used across seasons by ponderosa pine in northern Arizona. For Ecol Manage 289:425–433
Ketterings QM, Coe R, van Noordwijk M et al (2001) Reducing uncertainty in the use of allometric biomass equations for predicting above-ground tree biomass in mixed secondary forests. For Ecol Manage 146:199–209
Kovács B, Tinya F, Ódor P (2017) Stand structural drivers of microclimate in mature temperate mixed forests. Agric For Meteorol 234–235:11–21
LeBauer DS, Wang D, Richter KT et al (2013) Facilitating feedbacks between field measurements and ecosystem models. Ecol Monogr 83:133–154
Lenoir J, Hattab T, Pierre G (2017) Climatic microrefugia under anthropogenic climate change: implications for species redistribution. Ecography 40:253–266
Lorimer CG, Frelich LE (1989) A methodology for estimating canopy disturbance frequency and intensity in dense temperate forests. Can J Forest 19:651–663
Lu M, Zhou X, Yang Q et al (2012) Responses of ecosystem carbon cycle to experimental warming: a meta-analysis. Ecology 94(3):726–738
Lutz JA, Larson AJ, Swanson ME, Freund JA (2012) Ecological importance of large-diameter trees in a temperate mixed-conifer forest. PLoS One 7:e36131
Mackenzie DI, Royle JA (2005) Designing occupancy studies: general advice and allocating survey effort. J Appl Ecol 42:1105–1114
Mann ME, Bradley RS, Hughes MK (1998) Global-scale temperature patterns and climate forcing over the past six centuries. Nature 392:779–787
Nehrbass-Ahles C, Babst F, Klesse S et al (2014) The influence of sampling design on tree-ring-based quantification of forest growth. Global Change Biol 20:2867–2885
Nickless A, Scholes RJ, Archibald S (2011) A method for calculating the variance and confidence intervals for tree biomass estimates obtained from allometric equations. S Afr J Sci 107:86–95
Pacala SW, Canham CD, Saponara J et al (1996) Forest models defined by field measurements: estimation, error analysis and dynamics. Ecol Monogr 66:1–43
Pederson N, Dyer JM, McEwan RW (2014) The legacy of episodic climatic events in shaping temperate, broadleaf forests. Ecol Monogr 84:599–620
Poulter B, Frank D, Ciais P et al (2014) Contribution of semi-arid ecosystems to interannual variability of the global carbon cycle. Nature 509:600–603
PRISM Climate Group (2004) Oregon State University. http://prism.oregonstate.edu
Richardson AD, Williams M, Hollinger DY et al (2010) Estimating parameters of a forest ecosystem C model with measurements of stocks and fluxes as joint constraints. Oecologia 164:25–40
Rollinson CR, Kaye MW, Canham CD (2016) Interspecific variation in growth responses to climate and competition of five eastern tree species. Ecology 97:1003–1011
Rubino DL, McCarthy BC (2004) Comparative analysis of dendroecological methods used to assess disturbance events. Dendrochronologia 21:97–115
Shaver GR, Canadell J, CHAPIN FS III et al (2000) Global warming and terrestrial ecosystems: a conceptual framework for analysis. Bioscience 50:871–882
Slik JW, Paoli G, McGuire K, Amaral I (2013) Large trees drive forest aboveground biomass variation in moist lowland forests across the tropics. Glob Ecol Biogeogr 22:1261–1271
Speer JH (2010) Fundamentals of tree-ring research. U. of Arizona Press, Tucson.
St George S (2014) An overview of tree-ring width records across the Northern Hemisphere. Quatern Sci Rev 95:132–150
St George S, Ault TR (2014) The imprint of climate within Northern Hemisphere trees. Quatern Sci Rev 89:1–4
St George S, Meko DM, Cook ER (2010) The seasonality of precipitation signals embedded within the North American Drought Atlas. The Holocene 20:983–988
Stokes MA, Smiley TL (1968) An introduction to tree-ring dating. University of Chicago Press, Chicago
Swetnam TW, Lynch AM (1989) A tree-ring reconstruction of western spruce budworm history in the southern Rocky Mountains. Forest Sci 35:962–986
Swetnam TW, Allen CD, Betancourt JL (1999) Applied historical ecology: using the past to manage for the future. Ecol Appl 9:1189–1206
Touchan R, Allen CD, Swetnam TW (1996) Fire history and climatic patterns in ponderosa pine and mixed-conifer forests of the Jemez Mountains, northern New Mexico. U.S. Forest Service General Technical Report RM-GTR-286, pp 33–46
Touchan R, Woodhouse CA, Meko DM, Allen C (2011) Millennial precipitation reconstruction for the Jemez Mountains, New Mexico, reveals changing drought signal. Int J Climatol 31:896–906
van Mantgem PJ, Stephenson NL, Byrne JC et al (2009) Widespread increase of tree mortality rates in the western United States. Science 323:521–524
Weiner J (2004) Allocation, plasticity and allometry in plants. Perspect Plant Ecol Evol Syst 6:207–215
Williams AP, Allen CD, Macalady AK et al (2013) Temperature as a potent driver of regional forest drought stress and tree mortality. Nat Clim Change 3(3):292–297
Wood SN (2004) Stable and Efficient Multiple Smoothing Parameter Estimation for Generalized Additive Models. J Am Stat Assoc 99:673–686
Wood SN (2011) Fast stable restricted maximum likelihood and marginal likelihood estimation of semiparametric generalized linear models. J R Stat Soc B 73:3–36
Yamaguchi DK (2011) A simple method for cross-dating increment cores from living trees. Can J For Res 21:414–416
Yee TW, Mitchell ND (1991) Generalized additive models in plant ecology. J Veg Sci 2:587–602
(2012) Temperature as a potent driver of regional forest drought stress and tree mortality. 2:1–6